

16 January 2006

Contribution to Proceedings ICMS Workshop on Rogue Waves

12-15 December 2005, Edinburgh

Two preprints (submitted):

E. van Groesen, Andonowati & N. Karjanto:

Displaced Phase-Amplitude variables for waves on finite background

E. van Groesen & Andonowati

Finite energy wave signals of extremal amplitude in the spatial NLS equation

E. van Groesen (groesen@math.utwente.nl)

Applied Mathematics, University of Twente, Netherlands,
LabMath-Indonesia, Bandung Indonesia

Andonowati (aantrav@attglobal.net)

Applied Mathematics, University of Twente, Netherlands,
LabMath-Indonesia, Bandung Indonesia
Mathematics, Institut Teknologi Bandung, Indonesia

N. Karjanto (n.karjanto@math.utwente.nl)

Applied Mathematics, University of Twente, Netherlands



www.math.utwente.nl/aamp/



www.labmath-indonesia.or.id



Institut Teknologi Bandung

www.labmath-itb.or.id

Displaced Phase-Amplitude variables for Waves on Finite Background

E. van Groesen^{a,b,*} Andonowati^{a,b,c} N. Karjanto^a

^a*Department of Applied Mathematics, University of Twente, The Netherlands*

^b*LabMath-Indonesia, Bandung, Indonesia*

^c*Department of Mathematics, Institut Teknologi Bandung, Indonesia*

Abstract

Wave amplification in nonlinear dispersive wave equations may be caused by nonlinear focussing of waves from a certain background. In the model of Nonlinear Schrodinger equation we will introduce a transformation to displaced phase-amplitude variables with respect to a background of plane waves. The potential energy in the Hamiltonian then depends essentially on the phase. Looking as a special case to phases that are time independent, the oscillator equation for the signal at each position becomes autonomous, with the change of phase with position as only driving force for a spatial evolution towards extreme waves. This is observed to be the governing process of wave amplification in classes of known solutions of NLS, namely the Akhemediev-, Ma- and Peregrine solitons. We investigate the case of the Soliton on Finite Background in detail in this letter as the solution that describes the complete spatial evolution of modulational instability from background to extreme waves.

Key words: modulational instability, waves on finite background, displaced phase-amplitude, soliton solutions

PACS: 52.35.Mw, 46.40.Cd, 47.35.Bb, 47.54.Bd, 91.30.Fn, 05.45.Yv, 94.05.Pt

1 Introduction

Modulational instability is one of the processes that lead to amplification of background waves of small or moderate height into ‘extreme’ waves of large height (rogue or freak waves). The process, different from linear phase focussing, is essentially nonlinear. Since the full nonlinear evolution of the initial linear instability of a plane wave train, known as the Benjamin-Feir instability, is difficult to study for the full surface wave equations, we will use the simplified focussing NLS model for a thorough and full investigation.

* Corresponding author.

Email address: groesen@math.utwente.nl (E. van Groesen).

Despite much recent research [1–9], it is still rather unclear which circumstances are responsible for the appearance of an extreme wave from a certain background. One of the difficulties seems to be that the actual occurrence of extreme waves cannot be separated from the circumstances that are created by the background. Indeed, following ideas of Boccotti [10] it was shown in Craig [11] that the Draupner wave could have developed with linear evolution from the time signal at a much earlier time. In oceanographic situations with forcing by wind and current, a large variety of wave systems that can act as background will be produced. Knowledge of the properties of background wave fields that lead to extreme waves is therefore required. On the other hand, the study of the mathematical-physical properties of extreme waves is equally important since this may help to identify the characterization of backgrounds that are favourable for extreme waves.

In this paper we will address both aspects for uni-directional waves. Starting with an asymptotic wave field that is a modulated uniform wave train, we will study the full nonlinear evolution that leads to extreme waves. This is done by introducing suitable variables with respect to this background. These will be a kind of displaced phase-amplitude variables, with a displacement that depends on the background. Alternatively, they are the phase-amplitude variables for the complex amplitude of the difference with the background. Most important is that then the dynamics is governed by a Hamiltonian that contains a potential energy from the cubic nonlinearity and from quadratic contributions that depends explicitly on the phase variable itself.

Investigating special cases, we then restrict the phase to depend only on the position and not on time. Then the dynamics at each position is given as the motion of a nonlinear autonomous oscillator in a potential energy that depends on the phase as a parameter and on the spatial phase change. This change of phase with position, which physically corresponds to a change of the wavelength of the carrier wave, turns out to be the only driving force responsible for the nonlinear amplification towards an extreme wave. Remarkably, the assumption that the phase is independent of time leads necessarily to the well known special solutions of NLS, the Soliton on Finite Background [12–14], the Ma-solitons [15] and the algebraic Peregrine solution [16]. In this paper we will restrict to a detailed investigation of the SFB [17].

This investigation will give us a complete description of the full nonlinear process from small modulations to the extreme wave, and with that of the spatial development of the background in which the extreme wave appears. Calini and Schober [18] investigated this solution (and similar solutions with more unstable sidebands) in a dynamical system approach for persistence as a homoclinic orbit under perturbations. Such results are of paramount importance to study the robustness of the whole generation process.

Our analysis will show that actually a limited number of functionals seem to play a role in the complicated process. Since two of these functionals describe the physically relevant and well defined quantities of horizontal momentum and energy, the relevance of the optimization properties that we will find, may be relevant for other cases too. In fact, these functionals are nowadays also used in statistical descriptions [5,19,20].

The organization of the paper is as follows. Section 2 starts with some preliminaries to fix notation and introduce the variational formulations. Section 3 defines the transformation to displaced phase-amplitude variables, while section 4 specifies for phases independent of time. There the formulation of the evolution of the time signals is given as a family of constrained

optimization problems, and the special NLS-solutions are found. The Soliton on Finite Background is described and interpreted in physical variables in detail. The letter finishes with some remarks and conclusions.

2 Preliminaries

In this section we introduce the notation to be used, and in particular the variational aspects of NLS that will play a role in the following. We will also show how the most well known solutions of NLS are characterized directly in a variational way.

2.1 Variational descriptions for NLS

We consider real valued wave groups in space (x) and time (t): $\eta(x, t)$. In lowest order the wave group is described in the standard way as a monochromatic carrier wave with slowly varying complex amplitude A by:

$$\eta(x, t) = A(\xi, \tau) e^{i\theta_0} + cc, \quad \theta_0 = k_0 x - \omega_0 t, \quad k_0 = K(\omega_0)$$

where $\omega \rightarrow K(\omega)$ is the governing linear dispersion relation. To describe the space evolution for the signalling problem for NLS, we use a coordinate system with delayed time: $\xi = x, \tau = t - x/V_0$ where $V_0 = 1/K'(\omega_0)$ is the group velocity. Then A satisfies the NLS equation which can be written in the following way

$$i\partial_\xi A + \delta H(A) = 0,$$

where δH denotes the variational derivative of the Hamiltonian H which is given as a functional of functions of τ by

$$H = \int \left[\frac{1}{2} \beta |\partial_\tau A|^2 - \frac{\gamma}{4} |A|^4 \right] d\tau.$$

The parameter β is related to group velocity dispersion, and γ is related to the quadratic or third order nonlinearity in the equation for η . These coefficients depend on the center frequency ω_0 . For surface waves with sufficiently large carrier frequency ω_0 the parameters lead to the converging NLS for which $\beta\gamma > 0$; in the following we will assume this and take (without restriction) $\beta > 0, \gamma > 0$. Although it is possible to scale the variables so that $\beta = \gamma = 1$, we prefer to keep β and γ to identify which terms in the following are from dispersion and which from nonlinear effects.

Higher order terms have to be added to the first order expression above, but in the rest of this paper we will suppress these terms that are completely determined by A .

The NLS equation is written above in its Hamiltonian form. In the following it will be illustrative to perform transformations through the action principle which reads

$$\mathcal{A}(A) = \int \int \frac{1}{2} [iA^* \cdot \partial_\xi A] d\xi d\tau + \int H(A) d\xi$$

Besides the Hamiltonian, the horizontal momentum functional $\int |A|^2 d\tau$ is conserved (actually, there are infinitely many invariant integrals, but these two are most relevant for the following and from a physical point of view):

$$\partial_\xi H(A) = 0, \quad \partial_\xi \int |A|^2 d\tau = 0.$$

2.2 Phase amplitude description

The description with the complex amplitude A can be translated to phase-amplitude description by introducing polar coordinates:

$$A = ae^{i\psi}, \quad a \geq 0$$

The governing equations are most directly obtained from the action principle, which can be transformed (removing uninteresting total derivatives) into

$$\mathcal{A}(a, \psi) = \int \int \left[-\frac{1}{2} \{a^2 \partial_\xi \psi\} + \frac{1}{2} \beta a_\tau^2 + \frac{1}{2} \beta a^2 \psi_\tau^2 - \frac{\gamma}{4} a^4 \right] d\xi d\tau$$

Variations with respect to ψ leads to the energy equation

$$\partial_\xi [a^2] - \partial_\tau [\beta \psi_\tau a^2] = 0$$

while the phase equation results from variations with respect to a :

$$-a\psi_\xi - \beta a_{\tau\tau} + \beta a\psi_\tau^2 - \gamma a^3 = 0.$$

Remark 1 *In physical variables, the energy equation becomes*

$$\partial_x (a^2) + \partial_t \left(\frac{a^2}{V(k)} \right) = 0$$

and the phase equation becomes

$$\beta a_{\tau\tau} + (\psi_\xi - \beta \psi_\tau^2) a + \gamma a^3 = 0.$$

The phase equation can be recognized as the nonlinear dispersion relation NDR:

$$K(\omega) - k = \beta \frac{\partial_t^2 a}{a} + \gamma a^2$$

where the Chu-Mei quotient [21,22] (also called Fornberg-Whitham term [23,24]) $\beta \partial_t^2 a/a$ can be recognized.

For the following it is relevant to observe that the phase equation is actually an oscillator equation for the amplitude as function of τ :

$$\beta \partial_\tau^2 a + (\psi_\xi - \beta \psi_\tau^2) a + \gamma a^3 = 0.$$

At each position this oscillator equation is non-autonomous in general, and the linear term changes in time and with position through the coefficient $(\psi_\xi - \beta \psi_\tau^2)$, i.e. through the deviation from the linear dispersion relation $K(\omega) - k$.

The conservation of Hamiltonian and momentum now reads

$$\begin{aligned}\partial_\xi \int \left[\frac{1}{2} \beta a_\tau^2 + \frac{1}{2} \beta \psi_\tau^2 a^2 - \frac{\gamma}{4} a^4 \right] d\tau &= 0, \\ \partial_\xi \int a^2 d\tau &= 0.\end{aligned}$$

2.3 Nonlinear monochromatics and Solitons

As for many PDEs, special solutions can be obtained by separation of variables.

The nonlinear monochromatic solution changes the linear chromatic solution only in the dispersion relation; for a monochromatic wave of amplitude r_0 it is the solution

$$A = r_0 e^{-i\alpha\xi} \text{ with } \alpha = \gamma r_0^2$$

corresponding to the physical solution (in lowest order) $\eta = 2r_0 \cos((k_0 + \alpha)x - \omega_0 t)$. This shows that at the same frequency the wavenumber is modified, according to the nonlinear dispersion relation: $k = K(\omega_0) + \gamma a^2$ with $a = 2r_0$ the amplitude. This monochromatic train will be used as ‘background’ in the next sections. Other solutions of the form

$$A = S(\tau) e^{-i\alpha\xi}$$

can also be obtained. Substituting this expression in the equation there results as equation for the profile S :

$$\beta S_{\tau\tau} - \alpha S + \gamma S^3 = 0.$$

This is actually the phase equation, while the energy equation is trivially satisfied. Solutions exist for each $\alpha > 0$: it is the oscillator equation with effective potential energy

$$V(S) = -\alpha S^2/2 + \gamma S^4/4.$$

Since $\alpha > 0$, the origin is unstable, while boundedness is assured by the fourth order term. The equilibrium is the nonlinear monochromatic above; oscillations around this equilibrium describe modulations. The soliton is the homoclinic solution with $S(\tau) \rightarrow 0$ for $\tau \rightarrow \pm\infty$.

It can be observed that the governing equation for S can be found by substituting the Ansatz $A = S(\tau) e^{-i\alpha\xi}$ directly in the action principle, leading to

$$\int \int \left[\frac{1}{2} \alpha S^2 + \frac{\beta}{2} S_\tau^2 - \frac{\gamma}{4} S^4 \right] d\xi d\tau;$$

critical points with respect to S leads to the governing equation (rendering a formally divergent value to the integral). Stated differently, this can be interpreted as a constrained variational formulation of the momentum at level set of the Hamiltonian:

$$\min_S \left\{ \int \frac{1}{2} S^2 d\tau \mid H(S) = \gamma \right\}$$

where α is the (reciprocal) Lagrange multiplier. We will see a similar formulation in the next sections.

In the complex amplitude plane, the so-called Argand diagram, the solutions for each $\alpha > 0$ are depicted as follows. For each position $\xi (= x)$, the motion in the Argand plane is on a straight line through the origin with angle $-\alpha$, and the soliton solution is the motion homoclinic to the origin.

The physical wave fields corresponding to these solutions are given by

$$\eta(x, t) = 2S(t - x/V_0) \cos((k_0 - \alpha)x - \omega_0 t) + h.o.t.$$

It is to be noted that the carrier wave has fixed wavelength and period, whereas the solutions we will study in Section 4 will have wavenumber changing with position. For the soliton, the amplitude vanishes at $\xi = -\infty$, increases to a finite value for increasing ξ and vanishes towards $\xi \rightarrow \infty$. The periodic solutions describe modulations of the envelope around the amplitude value $2r_0$. For each of these solutions, at all fixed positions the time signal S is the same, with a delay at subsequent positions related to the propagation of the envelope. In contrast, the solutions in Section 4 will have different time signals at different positions.

3 Description of Waves on Finite Background

The solutions above are never associated with modulation instability: the soliton as homoclinic orbit has exponential growth and decay at infinity, and the modulated oscillation describes a periodic bounded motion. Modulational instability, with the Benjamin-Feir instability of wave trains in surface water waves as prime example, is commonly associated with finite amplitude wave trains that get amplified by self focussing processes due to modulations in the envelope amplitude. We will restrict in the following to this basic setting of a perturbation of a uniform wavetrain, although other ‘backgrounds’ deserve more attention too.

To define more precisely the class of waves we are interested in, we take as background a nonlinear harmonic (plane wave), $r_0 e^{-i\alpha\xi}$, with $\alpha = \gamma r_0^2$, and we will look for solutions of the form

$$A = B(\xi, \tau) r_0 e^{-i\alpha\xi},$$

where asymptotic properties for B will be specified further. For this asymptotic we will require that except for a possible phase factor, the asymptotic value is the plane wave, i.e. we require that

$$|B| \rightarrow 1 \text{ for } \xi \rightarrow \pm\infty \text{ or } \tau \rightarrow \pm\infty.$$

This asymptotic behaviour motivates, without putting additional restrictions, the introduction of reduced phase ϕ and amplitude G parameters according to

$$B = G(\tau, \xi) e^{i\phi(\xi, \tau)} - 1, \quad G, \phi \text{ real.}$$

The asymptotic requirement implies that $G - 2 \cos \phi \rightarrow 0$. In the cases below we will deal with solutions for which G_τ and $\phi_\tau \rightarrow 0$. Then for some limiting phases ϕ_\pm it holds that

$$\phi \rightarrow \phi_\pm \text{ and } G \rightarrow 2 \cos(\phi_\pm) \text{ asymptotically.}$$

In the complex (Argand) plane, these parameters are depicted in Fig. 1.

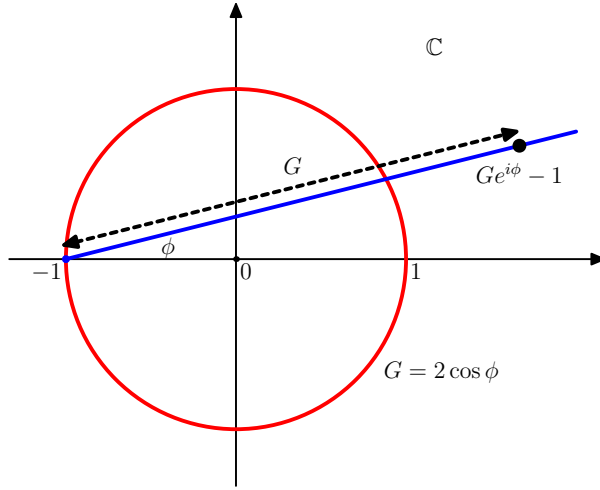


Fig. 1. In the Argand plane for the NLS amplitude, indicated are the displaced phase-amplitude parameters; the unit sphere corresponds to the set $G = 2 \cos \phi$.

To arrive at the governing phase-amplitude equations, we substitute $A = \left(G(\tau, \xi) e^{i\phi(\xi, \tau)} - 1 \right) r_0 e^{-i\alpha\xi}$ into the action functional and find:

$$\mathcal{A}(G, \phi) = r_0^2 \int d\xi \left[\int -\frac{1}{2} \phi_\xi G^2 d\tau + \bar{H}(G, \phi) \right]$$

where the transformed Hamiltonian reads

$$\bar{H}(G, \phi) = \int \left[\frac{\beta}{2} G_\tau^2 + \frac{\beta}{2} \phi_\tau^2 G^2 - W(G, \phi; \alpha) \right] d\tau$$

and where we have introduced the normalized potential energy as follows. The non-normalized expression for W is given explicitly by $-\alpha |Ge^{i\phi} - 1|^2 / 2 + \alpha |Ge^{i\phi} - 1|^4 / 4 = \alpha G^2 (G - 2 \cos \phi)^2 / 4 - \alpha / 4$. In the following we will discard the uninteresting constant term which, moreover, gives rise to divergence of the action functional, and take

$$W = \frac{\alpha}{4} G^2 (G - 2 \cos \phi)^2.$$

It is to be noted that W has, besides the origin $G = 0$, the unit circle in the complex plane as set of nontrivial critical points:

$$\frac{\partial W}{\partial G} = \frac{\partial W}{\partial \phi} = 0 \text{ for } G = 2 \cos \phi, \text{ for which } W = 0 \text{ and } |Ge^{i\phi} - 1| = 1.$$

The governing equations follow from variations with respect to ϕ and G . Variation with respect to $\phi(\xi, \tau)$ gives the (time integrated) energy equation which takes the form

$$\partial_\xi \left(\frac{1}{2} G^2 \right) - \partial_\tau (\beta \phi_\tau G^2) - \frac{\partial W}{\partial \phi} = 0$$

while variation with respect to $G(\xi, \tau)$ gives the ‘displaced’ phase equation

$$\phi_\xi G - \beta \phi_\tau^2 G + G_{\tau\tau} + \frac{\partial W}{\partial G} = 0.$$

The energy equation shows a forcing from the dependence of W on ϕ . The phase equation is the transformed nonlinear dispersion relation. It can again also be interpreted as a nonlinear oscillator equation for G , which now depends on ϕ through the dependence in W and on the combination of its derivatives $\phi_\xi - \beta\phi_\tau^2$ that contributes to the coefficient in front of the linear term. In general this is therefore a non autonomous oscillator equation. Note that it has exactly the same form as the general phase equation, but now W depends essentially on the phase ϕ . For fixed ϕ , the energy of each oscillator is therefore not constant in general, but for time periodic motions the time-integral over one period vanishes: there is no nett energy in- or output.

The conservation properties for the spatial evolution are now given by the momentum

$$\partial_\xi \int (G^2 - 2G \cos \phi + 1) d\tau = 0$$

and the original Hamiltonian

$$\partial_\xi \int \left[\frac{\beta}{2} (G_\tau^2 + \phi_\tau^2 G^2) - \frac{\alpha}{4} |Ge^{i\phi} - 1|^4 \right] d\tau = 0.$$

As a consequence, also the transformed Hamiltonian is conserved: $\partial_\xi \bar{H} = 0$. For solutions with the asymptotic as above, we have $W \rightarrow 0$ for $\xi \rightarrow \pm\infty$. Hence it follows that $\bar{H} = 0$ asymptotically, and then the constancy in ξ implies

$$\bar{H} = 0 \text{ for all } \xi.$$

Related to the non-autonomous character of the equation, in general, the dependence of ϕ on τ implies that at a fixed spatial position the motion in the Argand diagram is not on a straight line. In the next section we will consider special solutions for which the motion is at each position represented by a motion on a straight line, the line turning with position.

4 Pseudo-coherent wave solutions

In this section we consider special solutions for which the displaced phase ϕ does not depend on time. In the first section we show that then the spatial evolution is fully described by a family of constrained optimization problems for the time signals. Each optimization problem is only parameterized by the phase, and the spatial dynamics comes in from the change of the multiplier with phase. Remarkably, classes of solutions of these optimization problems can be found explicitly; the corresponding solutions found in this way are then recognized as well known NLS soliton-type solutions. In the next subsections the specifics are then given for the case of the soliton on Finite Background, referring to another paper for the other cases.

4.1 Parameterized constrained optimization for evolving time signals

From the assumption that the phase does not depend on time,

$$B = G(\tau, \xi) e^{i\phi(\xi)} - 1,$$

it follows that at each position the phase is constant, and the governing oscillator equation for G will be autonomous. Note that although the displaced phase ϕ is assumed to depend on ξ only, for the phase of the complex amplitude $B = be^{i\psi}$, ψ will depend on τ (and ξ), and therefore the NLS signal itself is not coherent; we will call this a pseudo-coherent solution, since it is coherent with respect to the displaced phase-amplitude variables.

The fact that the dependence on τ is missing in ϕ implies that the motions in the Argand plane are on straight lines through the point -1 , with angle ϕ that depends on the position $\xi(=x)$: the solution is displaced over a distance -1 in the complex plane.

The equations for G and ϕ are a special case of the above, but it is illustrative to derive them directly from the action principle, which now reads

$$\mathcal{A}(G, \phi) = r_0^2 \int d\xi \left[\int -\frac{1}{2} \phi_\xi G^2 d\tau + \bar{H}(G, \phi) \right]$$

with $\bar{H}(G, \phi) = \int \left[\frac{\beta}{2} G_\tau^2 - W(G, \phi; \alpha) \right] d\tau$

and with W as above.

Variation with respect to $\phi(\xi)$ gives the time integrated energy equation

$$\partial_\xi \int \frac{1}{2} (G^2) d\tau - \int \frac{\partial W}{\partial \phi} d\tau = 0$$

which shows the forcing from the dependence of the potential energy on the phase. Variation with respect to $G(\xi, \tau)$ gives the displaced phase equation

$$\phi_\xi G + \beta G_{\tau\tau} + \frac{\partial W}{\partial G} = 0.$$

This last equation shows that at fixed ξ the nonlinear oscillator equation for G depends on ϕ and ϕ_ξ but not on τ , so that at each position the equation for G is autonomous. An effective potential energy defined by

$$V = W + \frac{1}{2} \lambda G^2 = G^2 \left[\alpha^2 (G - 2 \cos \phi)^2 / 4 + \lambda / 2 \right]$$

is the oscillator potential for $\lambda = \partial_\xi \phi$. For negative λ the plots of the potential are depicted in Fig. 2.

The conservation properties for the spatial evolution are as before the momentum and the Hamiltonian; in particular

$$\bar{H} = \int \left(\frac{\beta}{2} G_\tau^2 - W \right) = 0 \text{ for all } \xi.$$

Inspection of the oscillator equation shows that the solutions of the oscillator equations can be obtained in the following, somewhat surprising, variational way, the idea of which is motivated by the terms in the action functional.

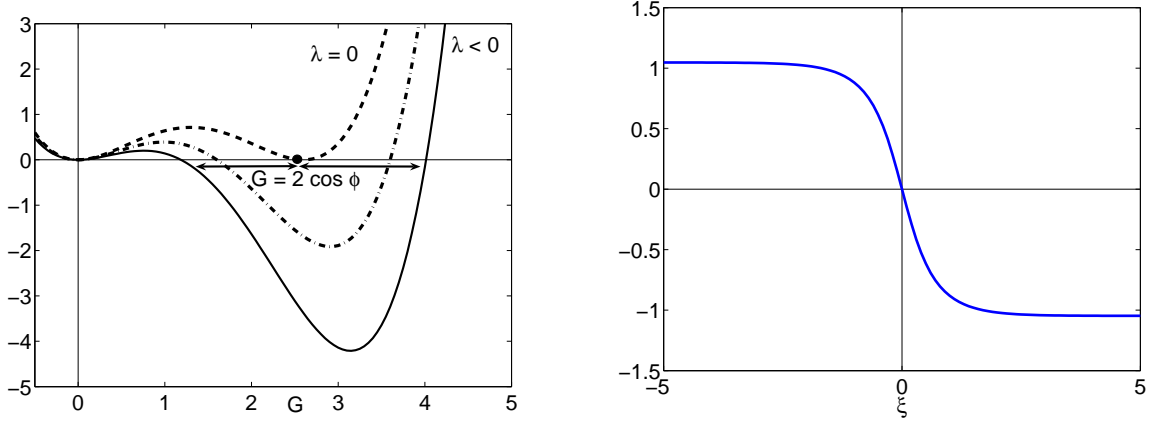


Fig. 2. (left) Shown are plots of the effective potential for various values of $\lambda < 0$. The dashed line is the plot for $\lambda = 0$. (right) The plot of the displaced phase of the SFB for $\tilde{\nu} = \sqrt{1/2}$.

Proposition 2 Consider for each ϕ the constrained variational problem

$$\text{Crit}_G \left\{ \int \frac{1}{2} G^2 \mid \bar{H}(G, \phi) = 0 \right\} \quad (1)$$

The nontrivial solutions $\tau \rightarrow \bar{G}(\phi)$ satisfy the Lagrange multiplier equation for some (reciprocal) multiplier $\lambda(\phi)$

$$\lambda G = \delta_G \bar{H}(G, \phi). \quad (2)$$

Then, if $\xi \rightarrow \phi(\xi)$ is a solution of the equation

$$\partial_\xi \phi = \lambda(\phi), \quad (3)$$

the spatial evolution $\xi \rightarrow \bar{G}(\phi(\xi))$ leads to a solution of the NLS equation given by

$$A = \left(G e^{i\phi(\xi)} - 1 \right) r_0 e^{-i\alpha\xi}. \quad (4)$$

The multiplier equation reads in detail

$$\partial_\tau^2 G + \lambda G + \alpha G(G - \cos \phi)(G - 2 \cos \phi) = 0 \quad (5)$$

and has linear, quadratic and cubic nonlinear terms. It is interesting that various classes of solutions of the constrained variational problem can actually be given explicitly and simply. All solutions are of the form

$$G = \frac{p}{q - \zeta(\tau)} \quad (6)$$

where p and q depend on ϕ and $\zeta(\tau)$ is one of three special functions, each of which corresponds to a well known special solution. For $\zeta(\tau) = \tau^2$ the solution is the well-known Peregrine (algebraic) soliton [16], while for $\zeta(\tau) = \cosh(\nu\tau)$ the solutions represent the class of Ma-solitons [15]. For $\zeta(\tau) = \cos(\nu\tau)$ the other well known ‘soliton on finite background’ [12–14] is obtained. We will present here the results for this last case since this describes the fully nonlinear spatial evolution of the Benjamin-Feir instability of a modulated monochromatic time signal. For the other cases we refer to [17].

Remark 3 In the variational formulation above, it is possible to take another target functional to be optimized:

$$\text{Crit}_G \left\{ \int G \mid \bar{H}(G, \phi) = 0 \right\}. \quad (7)$$

This is a consequence of the fact that the momentum is conserved, implying that

$$\int (G^2 - 2 \cos(\phi) G) = \text{constant}.$$

Of course the optimal solutions (and the multiplier) will be different, actually just a shift in \bar{G} . This last formulation, for the signal at the extreme position only, was proposed in [8,9].

4.2 Soliton on Finite Background

This class of solutions is, except for time and space shifts, a one parameter family depending on ν which is the modulation frequency of the background wave. The details are as follows.

Proposition 4 For any value of a modulation frequency ν such that $\tilde{\nu} := \nu\sqrt{\beta/\alpha} < \sqrt{2}$ the solution is given by

$$\bar{G}(\phi) = \frac{P(\phi)}{Q(\phi) - \cos(\nu\tau)}$$

where the coefficients are given by

$$P = \frac{\tilde{\nu}^2 Q}{\cos \phi}, \quad Q^2 = \frac{2 \cos^2 \phi}{2 \cos^2 \phi - \tilde{\nu}^2}$$

and the multiplier is given by

$$\lambda = (\tilde{\nu}^2 - 2 \cos^2 \phi) / \alpha.$$

Note that all solutions are periodic with the same period $T = 2\pi/\nu$.

The result can easily be verified by considering the function (6) with $\zeta(\tau) = \cos(\nu\tau)$:

$$f = \frac{p}{q - \cos(\nu\tau)}$$

Direct differentiation and algebraic manipulations show that this function satisfies an equation with linear, quadratic and cubic terms. Adjusting p, q in such a way that the coefficients are similar to those of the governing equation (5) leads to the expressions given above. The explicit spatial evolution is then found by solving $\partial_\xi \phi = \lambda = (\tilde{\nu}^2 - 2 \cos^2 \phi) / \alpha$ for ϕ as function of ξ . The result can be written in elementary functions:

$$\phi(\xi) = -\arctan \left[\frac{\sqrt{2 - \tilde{\nu}^2}}{\tilde{\nu}} \tanh(\sigma\xi) \right] \quad \text{where } \sigma = \alpha\tilde{\nu}\sqrt{2 - \tilde{\nu}^2}.$$

Note that the value of ν determines the asymptotic values of the phase:

$$\tilde{\nu} = \sqrt{2} \cos \phi_\pm$$

with $\phi_+ > \phi_-$ to assure that ϕ is decreasing. A characteristic plot of this function is given in Fig. 2.

Upon substituting all these results in the expression (4) leads after some algebraic manipulations to the solution that is known as the Soliton on Finite Background (SFB), described by [12–14]. We will present several observations about the physical process it describes, and the interpretation of the results in the next subsection.

Remark 5 *The SFB solution found here is modulated by one ‘sideband’ as we shall see. It is the first in an infinite series of solutions which are characterized by the number of sidebands. [14]. These SFB solutions are also described in [12,14,18,25].*

4.3 Interpretations

We will now illustrate the spatial evolution of the modulational instability described by SFB in various ways. It should be kept in mind that only first order effects are shown; when considering the NLS-model for surface wave phenomena, adding the second order bound waves will lead to some quantitative changes.

In the Argand diagram the time evolution is on a straight line through the ‘background’, under an angle that decreases for increasing position; this is illustrated for the case $\tilde{\nu} = \sqrt{1/2}$ in Fig. 3. Observe that only for $\xi = 0$, when the trajectory is on the real axis, the time signal is coherent.

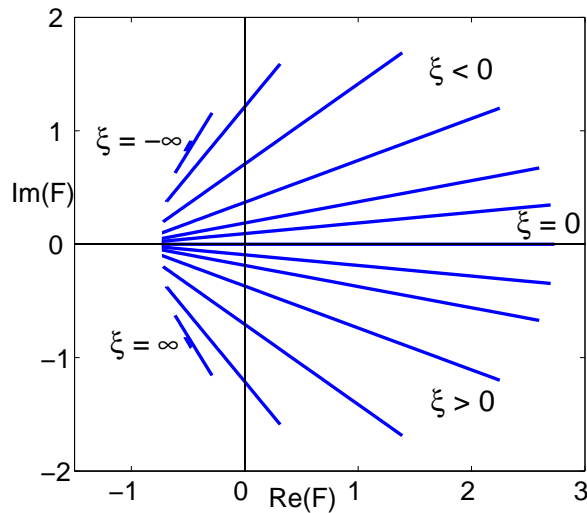


Fig. 3. The dynamic evolution of the SFB parameterized in τ at different ξ for $\tilde{\nu} = \sqrt{1/2}$.

The next plot, for the same values of the parameters, gives a snapshot of the spatial evolution which we will describe in some detail.

Fig. 4 shows the spatial wave field at some instant of waves, say, running from left to right. At the left the slightly modulated uniform wave train (amplitude $2r_0$) is seen. This modulation clearly determines a characteristic modulation length that is maintained during the complete downstream evolution. While moving to the right, the modulations are amplified, creating distinct wave groups. This initial phase is the so-called Benjamin-Feir instability [26]; the exponential growth rate from linear analysis depends on the value of ν and is given by the expression $\sigma = \sigma(\nu)$ above. After this initial exponential growth of the modulations, nonlinear effects come into play, enforce and later bound the increase in modulation amplitude. Till, at a certain position, called the *extreme position* (in scaled variables taken to be at $x = 0$), the largest wave appears, after which the reverse process sets in the decay towards the asymptotic harmonic wave train (with some phase change). Defining the amplification factor of the whole process as the quotient Q of the highest crest and the background amplitude, the amplification is larger

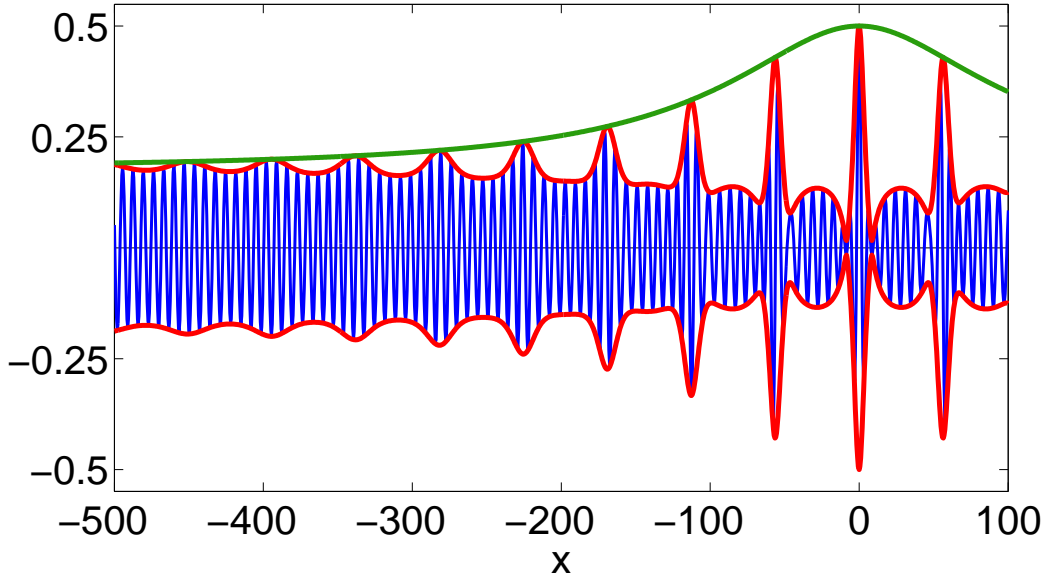


Fig. 4. Snapshot of the spatial wave field SFB for $\tilde{\nu} = \sqrt{1/2}$ and $\omega_0 = 3$ rad/sec. Shown are the individual waves, their envelope at that instant, and the time-independent MTA, maximal temporal amplitude. Physical dimensions are given along the axis: horizontally the distance and vertically the surface elevation in meters, for waves on a layer with depth of 5 meter. It is to be noted that this plot only shows the first order waves; adding second order bound waves will deform the waves and increase the MTA.

for smaller ν , maximal 3 (obtained in the limit $\tilde{\nu} \rightarrow 0$), as follows from the explicit expression given explicitly by [1,27] $Q = 1 + 2\sqrt{1 - \tilde{\nu}^2/2}$. Note that the local amplification factor near the extreme position can actually be much larger, since near the extreme position, the extreme wave is locally surrounded by waves of much smaller amplitude, as if the total energy in one wavegroup is conserved but with the energy redistributed between waves.

Dynamically in time, both the waves and the envelope shifts to the right at different speed (the phase and group velocity respectively). Also shown in the plot is the so-called MTA, the *maximal temporal amplitude* [28]. This is the (time-independent) curve determined by the maximal wave height at each point; it is the steady envelope of the wavegroups. This MTA is easily found from the explicit formulas above, by looking at bounds for G at each position:

$$2 \cos(\phi) - \frac{\sqrt{-2\lambda(\phi)}}{\alpha} \leq G(\tau, \phi) \leq 2 \cos(\phi) + \frac{\sqrt{-2\lambda(\phi)}}{\alpha}$$

The MTA then follows from $MTA(\xi)^2 = \max_{\tau} |Ge^{i\phi} - 1|^2$. Simplification of this expression leads to the result as in [8]

$$MTA(x)^2 = (2r_0)^2 \left[1 + \frac{2\tilde{\nu}^2 \sqrt{1 - \tilde{\nu}^2/2}}{\cosh(\sigma x) - \sqrt{1 - \tilde{\nu}^2/2}} \right]$$

In Fig. 5, the time signal at the extreme position is shown for the same values as above, to illustrate the appearance of phase singularities [29]. These correspond to wave dislocations of the spatial-temporal wave field, wave splitting and merging, and happens when the complex amplitude vanishes. This is the case (only at the extreme position) for sufficiently small values

of $\tilde{\nu}$, explicitly $0 < \tilde{\nu} < \sqrt{3/2}$; see [8,30].

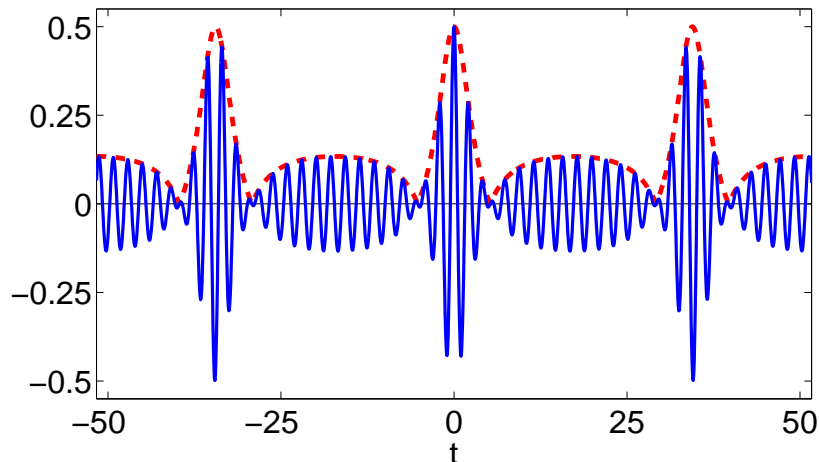


Fig. 5. Plot of the SFB signal at the extreme position for $\tilde{\nu} = \sqrt{1/2}$ and $\omega_0 = 3$ rad/sec.

5 Conclusion and remarks

We have investigated in this letter a specific, simple, ‘finite background’ and introduced displaced phase-amplitude variables to look for waves deviating from this background. We found the special known NLS-solutions by assuming the phase not to depend on time explicitly. This leads to a variational characterization of the time signals at each position; the change in phase with position drives the modulational instability process in these cases. The time signal at the position where the extreme waves appear, corresponds to a coherent solution, at other positions this is not the case. Conservation of horizontal momentum and of the Hamiltonian are essential in the described processes. Therefore it may be expected that some of the results can be carried over to models that approximate the full surface wave equations more precisely than NLS to show similar properties. An investigation guided by the formulation with an action principle seems most promising.

As a side result we found the characteristic wave forms for the time signals (6); it turns out that these, fully nonlinear profiles are a nonlinear modification of cornered waveforms that are obtained by changing the Hamiltonian to a quadratic expression and looking for waves with maximal crest height; see [31] for further details for finite energy and [32] for time periodic signals.

Acknowledgement

This work is executed at University of Twente, The Netherlands as part of the project “*Prediction and generation of deterministic extreme waves in hydrodynamic laboratories*” (TWI.5374) of the Netherlands Organization of Scientific Research NWO, subdivision Applied Sciences STW.

References

- [1] A.R. Osborne, M. Onorato, and M. Serio, *Phys. Lett. A* 275 (2000) 386.
- [2] K.L. Henderson, D.H. Peregrine, and J.W. Dold, *Wave Motion* 29 (1999) 341.
- [3] K.B. Dysthe and K. Trulsen, *Phys. Scripta* T82 (1999) 48.
- [4] K.B. Dysthe, *Proc. Rogue Waves*, 2000.
- [5] P.A.E.M. Janssen, *J. Phys. Ocean.* 33 (2003) 863.
- [6] A.R. Osborne, *Mar. Struct.* 14 (2001) 275.
- [7] M. Onorato, A.R. Osborne, M. Serio, and S. Bertone, *Phys. Rev. Lett.* 86 (2001) 5831.
- [8] Andonowati, N. Karjanto and E. van Groesen, Extreme wave phenomena in down-stream running modulated waves, submitted to *Applied Mathematical Modelling* (2004).
- [9] E. van Groesen, Andonowati, and N. Karjanto, *Proc. Rogue Waves* 2004.
- [10] P. Boccotti, *Ocean Engng.* 24 (1997) 265.
- [11] Craig et. al. submitted to *Phys. of Fluid*, 2005.
- [12] N.N. Akhmediev, V.M. Eleonskii, and N.E. Kulagin, *Sov. Phys. JETP* 62 (1985) 894.
- [13] N.N. Akhmediev, V.M. Eleonskii, and N.E. Kulagin, *Theor. Math. Phys.* 72 (1987) 183.
- [14] N.N. Akhmediev and A. Ankiewicz, *Solitons–Nonlinear Pulses and Beams* volume 5 of *Optical and Quantum Electronic Series*, Chapman & Hall, London, first edition, 1997.
- [15] Y.-C. Ma, *Stud. Appl. Math.* 60 (1979), 43.
- [16] D.H. Peregrine, *J. Austr. Math. Soc. Ser. B* 25 (1983) 16.
- [17] N. Karjanto and E. van Groesen, Relation among breather type solutions of the NLS equation, in preparation, 2006.
- [18] A. Calini and C.M. Schober, *Phys. Lett. A* 298 (2002) 335.
- [19] F. Fedele and F. Arena, *Phys. Fluids* 17 (2005) 026601.
- [20] F. Fedele, *Prob. Engng. Mech.* (2004).
- [21] V.H. Chu and C.C. Mei, *J. Fluid Mech.* 41 (1970) 873.
- [22] V.H. Chu and C.C. Mei, *J. Fluid Mech.* 47 (1971) 337.
- [23] E. Infeld and G. Rowlands, *Nonlinear waves, solitons and chaos*, Cambridge University Press, Cambridge, p 117–9, 1990.
- [24] V. Fornberg and G.B. Whitham, *Phil. Trans. R. Soc. Lond. A* 289 (1978) 373.
- [25] N.N. Akhmediev and N.V. Mitzkevich, *IEEE J. Quantum Elec.* 27 (1991) 849.
- [26] T.B. Benjamin and J.E. Feir, *J. Fluid Mech.* 27 (1967) 417.
- [27] N. Karjanto, E. van Groesen, P. Peterson, *J. Ind. Math. Soc.* 8 (2002) 39.
- [28] Andonowati and E. van Groesen, *J. Nonlinear Opt. Phys. Material* 12 (2003) 221.

- [29] J.F. Nye and M.V. Berry, Proc. R. Soc. Lond. A 336 (1974) 165.
- [30] N. Karjanto and E. van Groesen to be submitted to New Phys. J. 2006.
- [31] E. van Groesen and Andonowati, Finite energy wave signals of extremal amplitude in the spatial NLS-dynamics, submitted to Phys. Lett. A (2006).
- [32] E. van Groesen and Andonowati, Periodic wave signals of extreme crest height, in preparation (2006).

Finite energy wave signals of extremal amplitude in the spatial NLS-dynamics

E. van Groesen^{a,b,*} Andonowati^{a,b,c}

^a*Department of Applied Mathematics, University of Twente, The Netherlands*

^b*LabMath-Indonesia, Bandung, Indonesia*

^c*Department of Mathematics, Institut Teknologi Bandung, Indonesia*

Abstract

With the aim to find extremal properties of extreme waves, we consider waves of maximal crest (and wave) height in the model of the spatial NLS-dynamics. Using the two motion invariants momentum and Hamiltonian as constraints, we show that so-called cornered solitons provide the maximal crest heights for most pairs of feasible constraint values. At the boundary of the feasible set the well-known smooth solitons are found. We discuss the implications for the solutions of NLS evolving from an initial signal.

Key words: extreme waves, soliton, extremal properties, NLS equation

PACS: 52.35.Mw, 46.40.Cd, 47.35.Bb, 47.54.Bd, 91.30.Fn, 05.45.Yv, 94.05.Pt

1 Introduction

Recently there is much interest in extreme waves, also called rogue, or freak waves; see e.g. [1-10]. The aim is to find how waves with exceptionally high wave crest, or exceptionally large wave height, can arise within a wavefield of waves of moderate height. Linear dispersive focussing, or nonlinear self-focussing, or external influences (currents, winds, geometry or bathymetry) may be possible causes. A major question remains if, when external influences are excluded, extreme events are statistically accidental occurrences, or that specific mathematical-physical principles underly their generation.

In this contribution we provide a contribution to the understanding of extreme waves by considering for a specific evolution equation the question if an extreme wave event has some extremality property. By this we mean that the wave signal at the position where the highest wave occurs, can in some way be characterised as the signal that maximises the height of the

* Corresponding author.

Email address: groesen@math.utwente.nl (E. van Groesen).

wave crest compared to other signals that satisfy certain constraints. Of course, the set of competing signals, the specification of the constraints, has to be physically motivated or at least understandable.

If the physical wave elevation is denoted by $\eta(x, t)$, and the time signal at the extreme position by $s(t)$, the general formulation for extremal time signals is to find the profile with maximal crest height subject to given constraints. For real valued time signals the maximal crest height is defined as a functional for a signal by

$$C(s) := \max_t (s(t)),$$

and the extremal problem can be written as

$$\max_s \{ C(s) \mid \text{constraints } (s) \}.$$

Note that a similar reasoning applies for initial value problems when we investigate the wave profile at the instant at which the extreme height occurs; for compactness of writing we will consider the signalling problem: how a wave signal evolves in one spatial dimension. In this paper we restrict to signals defined on the whole real line with finite energy; a similar analysis has been excuted for time periodic signals, see [11].

In Section 2 we recall the property that a signal that has largest crest height among those of given powerspectrum will be a coherent signal. Then the extremal problem will be investigated for functional constraints, prescribed value for integrated densities. The derivative of the crest height functional leads in the governing equation to a Dirac delta function at the instant of the heighest crest. This will generally result in the appearance of corners in the optimal signal profile; smooth solutions can be obtained as limiting cases for constraint values for which the constraints are linearly dependent. After some general remarks, we illustrate this with cornered exponentials, a problem that can be seen as a linear version of the cornered soliton profiles of the next section. In Section 3 we consider first the well known NLS-soliton solutions and introduce cornered soliton signals which are the extremal crest signals when momentum and Hamiltonian (related to the physical energy) are prescribed. The solitons are the smooth limits of the cornered solitons, obtained at the boundary in the parameter space of the feasible constraint values. From these results we conclude that the standard soliton is the coherent signal that has largest wave crest when compared to all other signals with the same values for these dynamically invariant integrals, and that cornered solitons are the maximal amplitude solutions for other values of momentum and Hamiltonian. This rather appealing result does not seem to have been reported in the literature. Since both momentum and Hamiltonian, determined by the intial signal, are invariant for the NLS dynamics, these results have direct implications for the possible development from any intial signal; some of these dynamical implications of the results are investigated. In the concluding section 4 we report on related work and possible extensions. In particular we note that any reasonable model for surface waves will have such invariant functionals, which could imply that similar results are valid for more accurate descriptions too.

2 Extremal time signals

We start this section with the observation that a signal that has largest crest height among those of given powerspectrum will be a coherent signal. Prescribing the power spectrum is very

restrictive, much more restrictive than prescribing its total integrated energy for instance. That is the motivation to investigate extreme signals when integral constraints are prescribed. The crest height functional leads to a Dirac delta function at the instant of the highest crest, which results in corners in the optimal signal profile. After some general remarks, we illustrate this for finite energy signals on the whole real line with a problem that can be seen as a linear version of the cornered soliton profiles that we will encounter in the next section.

2.1 Prescribed power spectrum

Signals for which the quadratic powerspectrum is given, say $S(\omega)$, are all of the form

$$s(t) = \int \sqrt{S(\omega)} e^{i\Phi(t)} d\omega$$

for some phase function $\Phi(t)$. Clearly the signal has maximal crest height if all phases are the same, say $\Phi = 0$ to get a real valued signal:

$$s_{ext}(t) = \int \sqrt{S(\omega)} d\omega$$

This is the well know result for a fully coherent signal. Evolving this signal with a *linear* dispersive wave equation will not change the spectrum, but will lead to dispersive decay of the maximal crest height at other positions. A characteristic example is a Gausssian spectrum evolving according to the linear NLS equation. The Maximal Temporal Amplitude [12], the curve of maximal crest heights at different positions, can be found explicitly and has square root asymptotic decay with distance.

In practical situations where the power spectrum can be obtained from measurements, evolving the coherent state in a linear way was called the ‘new wave’ in Craig e.a.[13] where its usefulness was demonstrated for the Draupner wave.

2.2 Integral constraints

The general formulation for the optimization of the crest height is now considered for constraints of functional type (integrated densities), say

$$\max_s \{ C(s) \mid s \in \mathcal{M} \}$$

where the constraint set is given by

$$\mathcal{M} = \{ s \mid F(s) = \gamma \}$$

for one or more functionals $F(s)$ of the time signal. The Langrange Multiplier Rule from standard variational calculus leads to the result that an optimal signal satisfies the following equation for some (vector) multiplier λ

$$\sigma \delta_{Dirac}(t - t_{\max}) = \lambda \delta F(s)$$

where t_{\max} is the time at which the highest wave crest occurs. We can distinguish two cases, depending on whether the constraint set is singular or not. A singular point of the constraint set is a point \bar{s} for which the functionals are dependent, i.e. for which for some nonvanishing vector λ it holds that $\lambda \delta F(\bar{s}) = 0$. This satisfies the multiplier equation for $\sigma = 0$. In that case the constraint set is called singular, and the specific values γ are called singular values. If there are no singular points, the constraint set is called regular.

For a regular constraint set, a critical point will satisfy the LMR for some nonzero σ , which can then be normalised to one, $\sigma = 1$. In most of the relevant cases, the Dirac delta function will cause the optimal profile to have a corner at the extremal time t_{\max} .

As a simple example, consider a quadratic constraint which will lead to linear equations. For the quadratic functional

$$F(\eta) = \frac{1}{2} \int L\eta \cdot \eta dt$$

where L is some (dispersion) operator, it holds that $\delta F(s) = Ls$ and the equation becomes

$$\sigma \delta_{Dirac}(t - t_{\max}) = \lambda Ls.$$

If L is nonsingular, all constraint sets with $\gamma \neq 0$ are regular, and hence $\sigma \neq 0$. Fourier transformation of the equation (taking $t_{\max} = 0$) shows that the solution has amplitude spectrum

$$\hat{s} = \frac{1}{\hat{L}(\omega)}.$$

The powerspectrum is given by $S(\omega) = |\hat{L}(\omega)|^{-2}$ and decays at infinity for coercive operators. If L is singular, say $L(s_0) = 0$, the maximization problem has no solution and crest heights can become arbitrarily large for each value of γ .

Remark 1 *In the next subsection we will deal with a combination of two quadratic functionals, for which L will become of the form $L = -\lambda_1 \partial_t^2 - \lambda_2$; the related power spectrum then has fourth order decay at infinity: $S(\omega) = (\lambda_1 \omega^2 + \lambda_2)^{-2}$, which seems quite reasonable for decaying wave turbulence.*

2.3 Exponential profiles with corners

To prepare for the NLS soliton to be treated in the next section, we now investigate optimal signals on the whole real line that vanish at infinity, so called finite energy signals. We will use the momentum functional M and the ‘quadratic energy’ functional E which may be seen as a simplified (quadratic) version of the NLS-Hamiltonian of the next section:

$$M(s) = \int \frac{1}{2} s^2, \quad E(s) = \int \frac{1}{2} (\partial_t s)^2.$$

The constraint sets to be considered are then for parameters $\gamma_M, \gamma_E \geq 0$

$$\mathcal{M} = \{ s \mid M(s) = \gamma_M, \quad E(s) = \gamma_E \}.$$

The governing equation is

$$\sigma \delta_{Dirac}(t - t_{\max}) = (\lambda_M - \lambda_E \partial_t^2) \eta$$

For any pair of positive constraint values γ_M, γ_E the set \mathcal{M} is nonempty and regular. Taking $t_{\max} = 0$ without restriction, the solutions are exponential functions that meet at a corner at $t = 0$

$$s_{\text{exp}} = ce^{-\mu|t|}$$

where c and $\mu > 0$ are determined by the constraint values. In fact, $M(s_{\text{exp}}) = c^2/\mu$ and $E(s_{\text{exp}}) = c^2\mu$. For normalised momentum and increasing γ_E the crest height c and the steepness at the corner $c\mu$ increase monotonically without bound.

3 Extremal wave height property of NLS cornered solitons

In the following we will take as simplified model the NLS equation for wave propagation in one spatial dimension. We will use Hamiltonian formulation of this equation since this is closest to the extremal descriptions we are after. Wave groups are described in the standard way as a monochromatic carrier wave with slowly varying complex amplitude A . This means that the complexified wave elevation is given in lowest order by

$$\eta_c(x, t) = A(\xi, \tau) e^{i\theta_0}, \quad \text{with } \theta_0 = k_0x - \omega_0t, \quad k_0 = K(\omega_0),$$

where $\omega \rightarrow K(\omega)$ is the governing linear dispersion relation. Here and in the following we will only consider this first order contribution, neglecting second order bound waves. Then maximal values of the complex amplitude may not precisely correspond to maximal value of η because of the presence of the carrier wave. We will not take this effect into account in the following, so that we actually deal with the the problem to characterise the extreme points of the envelope.

To describe the space evolution for the signalling problem for NLS, we use a coordinate system with delayed time: $\xi = x, \tau = t - x/V_0$ where $V_0 = 1/K'(\omega_0)$ is the group velocity. Then the NLS equation for A can be written in Hamiltonian form as

$$i\partial_\xi A + \delta H(A) = 0.$$

The Hamiltonian will depend on the carrier frequency. Restricting to the converging NLS equation for surface waves with sufficiently large carrier frequency ω_0 , we will take a suitably normalised Hamiltonian H that is given as a functional of functions of τ by

$$H = \int \left[\frac{1}{2} |\partial_\tau A|^2 - \frac{1}{4} |A|^4 \right] d\tau. \quad (1)$$

In the following we will also extensively use the momentum functional

$$M(A) = \int \frac{1}{2} |A|^2,$$

which is an invariant functional for the NLS evolution as a consequence of translation symmetry of the original water wave problem.

Prescribing the powerspectrum as we did in the previous section is a very restrictive constraint: the optimum is sought for variations in the phase only. The resulting coherency requirement of the signal is a property that is met also in many of the best known special solutions of nonlinear wave models, which is why they are often referred to as ‘coherent states’. In general the spectrum will change for nonlinear evolution. However, for some of such solutions the spectrum does not change at all during the evolution. This is the case, for instance, for the standard translating soliton and the soliton wave group of NLS, and the periodic equivalents. These are solutions that are characterised by the fact that the time signal is the same at each position, except from a time delay or phase factor. Such kind of solutions are relative equilibria of the Hamiltonian evolution equations. As such they have a dynamically well defined extremal formulation, namely they are critical points of the Hamiltonian when restricted to level sets of the momentum integral (see e.g. [14]). We will summarise this in the first subsection. In the next one we will show that the extremal problem for the amplitude with momentum and NLS-Hamiltonian as constraints lead in general to ‘cornered solitons’, while the smooth solitons are found on the boundary in parameter space of the constraint values. The dynamic consequences of these extremality results are then discussed.

3.1 Extremal formulation of the soliton

The NLS soliton wave group signal is obtained for a specified value of the momentum as the minimizer of the Hamiltonian

$$\min_s \{ H(A) \mid M(A) = \gamma_M \}. \quad (2)$$

Solutions are coherent states: a real time signal multiplied by an arbitrary phase function. It is therefore sufficient to look for the real signal, which is a solution of

$$h(\gamma_M) := \min_s \{ H(s) \mid M(s) = \gamma_M \} \quad (3)$$

For later reference we denoted the value of the energy of the soliton by the value function $h(\gamma_M)$. The governing equation, with λ as multiplier,

$$-\partial_\tau^2 s - s^3 = \lambda s$$

leads to the well known explicit expression

$$S(\tau) = \frac{a\sqrt{2}}{\cosh(a\tau)} \quad (4)$$

for $\lambda = -a^2$ where the parameter a is in a one to one relation with the value of the momentum: $\gamma_M = 4a$. The value of the Hamiltonian is then given by $H(S) = -\frac{4}{3}a^3$ and hence the value function and the multiplier are given by

$$h(\gamma_m) = -\frac{1}{48}\gamma_m^3, \quad \lambda = -\frac{1}{16}\gamma_m^2.$$

Corresponding to the soliton profiles are the actual soliton solutions of the NLS equation, given as the relative equilibrium solutions

$$A_{sol} = S(\tau) e^{i\phi_0} e^{i\lambda\xi}$$

where $e^{i\lambda\xi}$ is the action of the momentum flow and ϕ_0 an arbitrary phase.

This clearly shows that the nonlinear evolution does not change the power spectrum for these special solutions. Note, also, that the momentum flow is different from the NLS-linearized flow: the MTA for the soliton solution is constant, but when evolving the signal according to the linear dispersion, the MTA will show dispersive decay as described above.

This example of solitons as coherent states serves as a motivation to look for extremal formulations for the crest height (wave envelope) using dynamically relevant functionals as constraints, in particular integrals of the motion. Although NLS has infinitely many invariant integrals, we will exploit in the following only the two which have most physical relevance, the Hamiltonian and the momentum. The results may therefore be generalised to other conservative models with translation symmetry for which such basic invariant integrals exist.

3.2 Cornered solitons

The value function for the solitons $\gamma_H = h(\gamma_M)$ corresponds to a ‘soliton curve’ in the 2D parameter space with values of momentum and Hamiltonian (M, H) along the axis. All signals s will correspond to points in this plane on or above this curve: $H(s) \geq h(M(s))$. We will now show that all points above this curve have a ‘cornered soliton’ as the signal with largest envelope height.

To that end consider the following constrained optimization for the envelope:

$$\max_A \left\{ \max_{\tau} |A(\tau)| \mid M(A) = \gamma_M, \quad H(A) = \gamma_H \right\}.$$

When writing the complex amplitude signal as a real coherent signal s times a complex exponential, $A = s(\tau) e^{i\Phi(\tau)}$, it is seen that $M(A) = M(s)$ and $H(A) = H(s)$ so that we have essentially a problem for the (real) coherent part:

$$\max_s \{ C(s) \mid M(s) = \gamma_M, \quad H(s) = \gamma_H \}.$$

With any solution s_0 of this real problem, the solutions for the complex amplitude are simply all other coherent states: $A_0 = s_0 e^{i\phi}$ for some fixed ϕ .

It is interesting that we can find the solutions of this optimization problem.

The smooth NLS-solitons are encountered for values of the constraints for which the constraint set is singular, i.e. when the constraint values are on the soliton curve $\gamma_H = h(\gamma_M)$. Above this curve, the constraint set is regular, and the equation reads

$$\begin{aligned} \delta_{Dirac}(t - t_{\max}) &= \lambda_M \delta M + \lambda_H \delta H \\ &= \lambda_M s + \lambda_H \left(-\partial_t^2 s - s^3 \right) \end{aligned}$$

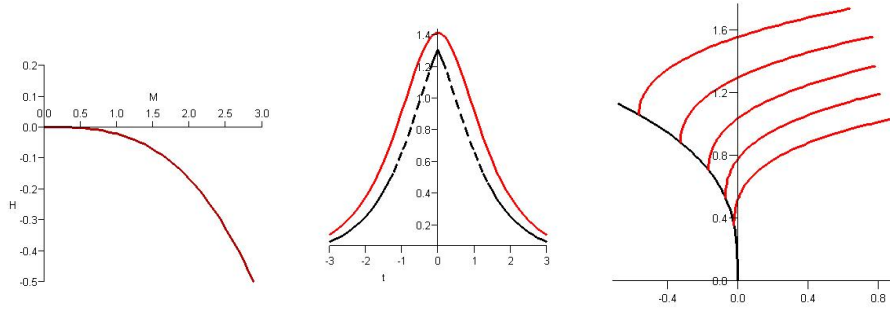


Fig. 1. The left figure is the plot of the soliton curve: the values of momentum M and Hamiltonian H for the solitons, i.e. the value function of the constrained optimization problem (3). All signals will have values M, H that correspond to points above this curve. The middle picture shows the graphs of the soliton with $a = 1$ and the cornered soliton with $b = a, \rho = 0, 4$ and shows the property of the cornered soliton as consisting of the tails of the soliton. The right plot shows crestheights as function of H . The dashed line is the crestheight for the soliton, and the other curves are the crestheights of cornered solitons at fixed M , from the lowest to the highest curve for $M = 1, 3/2, 2, 5/2, 3$.

Compared to the formulation of the cornered exponentials in the previous section, the quadratic energy constraint is replaced by a constraint on the NLS-Hamiltonian. As a consequence, cornered solitons are the solutions of the optimization problem; each cornered soliton is symmetric and consists of the tails of a smooth soliton that are glued together to make the correct corner condition. Hence, for this nonlinear case, the exponential tails of the cornered exponentials are now replaced by the tails of the NLS-soliton.

Cornered solitons, with corner at the origin, are explicitly given for parameters $b, \rho > 0$ by

$$S_c(b, \rho) = \frac{\sqrt{2}b}{\cosh(b(|\tau| + \rho))};$$

the soliton is recovered for $\rho = 0$. The momentum and Hamiltonian of these cornered solitons can be found explicitly:

$$M(S_c) = \frac{8b}{\exp(2b\rho) + 1}, \quad H(S_c) = -\frac{8b^3}{3} \frac{(-3 \exp(4b\rho) + 6 \exp(2b\rho) + 1)}{(\exp(2b\rho) + 1)^3}.$$

These expressions provide a one-to-one relation between the parameters b, ρ and the admissible values of momentum and Hamiltonian. The crest height of a cornered soliton is given by

$$C(S_c) = \frac{\sqrt{2}b}{\cosh(b\rho)}.$$

Resuming the above we have the following result.

Proposition 2 *The NLS-soliton signal has the largest envelope value compared to all other signals that have the same value of momentum and Hamiltonian as that soliton. For all other values of momentum and Hamiltonian, the cornered soliton with these values is the profile with maximal envelope.*

3.3 Dynamic relevance

Let us now look at the consequence of the results of the previous subsection for the evolution properties of the NLS equation.

A complex signal $A_0(t) = s_0(t) e^{i\phi_0(t)}$ at some initial position, say $\xi = 0$, determines $h_0 = H(A_0) = H(s_0)$ and $m_0 = M(A_0) = M(s_0)$. These values of momentum and Hamiltonian, being invariant integrals, remain constant during (unperturbed) Hamiltonian evolution.

If the values are on the soliton curve, i.e. $h(m_0) = h_0$, and if the complex signal is coherent ($\phi_0(\tau) = \phi_0 = \text{constant}$) $A_0 = S(\tau) e^{i\phi_0}$, the initial signal is actually a soliton signal. Then the evolution as relative equilibrium is very special and we get the spatial NLS soliton. Only such coherent signals are on the soliton trajectory that is given by $A(\xi, \tau) = S(\tau) e^{i\phi_0} e^{i\lambda\xi}$ with $\lambda = -m_0^2/16$. Hence, if the complex signal is not coherent ($\phi_0(\tau) \neq \text{constant}$), the evolution will never lead to a soliton signal, and the maximal crest height will remain lower than the soliton crest height.

In any other case that the initial signal is NOT a soliton, the Hamiltonian evolution will change the signal.

For values (m_0, h_0) above the soliton curve $h(m_0) < h_0$, the coherent cornered soliton, $A_0 = S_c(\tau) e^{i\phi_0}$ for some constant ϕ_0 , has the maximal amplitude among all other signals at (m_0, h_0) . Hence if the initial signal is such a coherent cornered soliton, the maximal waveheight over time and space is found at the initial position; the spatial dispersive evolution will initially decrease the maximal crest height and dispersively smoothen the corner.

If the initial signal is not a coherent soliton, nor a coherent cornered soliton, the evolution may possibly lead to a cornered soliton at some other position in space; this will happen when the initial signal is on the evolution trajectory of a cornered soliton. It seems impossible to characterise the evolution of a non-coherent soliton signal, or of a cornered soliton, in more detail theoretically.

Remark 3 *Evolution from any coherent state, so in particular from the cornered soliton signals, changes the power spectrum only in quadratic order with the distance (the spectrum for the soliton doesn't change at all). This was detailed in [9], and can be seen by Taylor expansion in ξ using the evolution equation*

$$A(\xi, \tau) = A_0(\tau) + i\xi\delta H(A_0(\tau)) + O(\xi^2).$$

If $A_0 = s(\tau) e^{i\phi_0}$, with s real, then also $\delta H(A_0) = \delta H(s) e^{i\phi_0}$, and hence the quadratic power spectrum becomes for small ξ (using a hat for Fourier transform)

$$|\hat{A}|^2 = |\hat{A}_0|^2 + O(\xi^2).$$

4 Conclusions and extensions

To find the signals of extreme crest height, we essentially used only two conserved integrals of NLS, the momentum and Hamiltonian, as constraints and found the coherent (cornered) soliton signals as extremals. This indicates that the result seems rather robust, since other model equations that describe the surface wave problem in higher accuracy will have these basic properties: the Hamiltonian structure inherited from that of the full problem, and momentum conservation from translation symmetry.

In this paper we did not investigate the evolution of the cornered soliton signals, nor of the non-coherent (cornered) solitons; numerical calculations will be reported elsewhere.

In practise, when measuring time signals of the water elevation, the signal can be used to calculate the momentum and Hamiltonian (after subtracting second order bound waves). It would be interesting to see how close evidently extreme waves in such a signal are to a coherent cornered soliton signal. As an approximation one may also directly compare the measurement with the cornered soliton shapes described here. Since in general measurements will not be for finite energy signals on the whole real line, it is worthwhile to mention that the characteristic cornered signals also appear in time periodic cases. In fact, similar investigations have been reported in [11] for periodic time signals that appear in a modulational instability process leading to extreme waves. Taking the whole spatial evolution into account it was shown that only the extreme signal is coherent, but not so the signals at other positions, which have vividly changing spectrum with distance.

As stated before, similar results can be obtained for the initial value problem of NLS for the temporal evolution of spatial wave forms.

Acknowledgement

This work is part of project TWI.5374 of the Netherlands Organization of Scientific Research NWO, subdivision Applied Sciences STW.

References

- [1] A.R. Osborne, M. Onorato, and M. Serio, *Phys. Lett. A* 275 (2000) 386.
- [2] K.L. Henderson, D.H. Peregrine, and J.W. Dold, *Wave Motion* 29 (1999) 341.
- [3] K.B. Dysthe and K. Trulsen, *Phys. Scripta* T82 (1999) 48.
- [4] K.B. Dysthe, *Proc. Rogue Waves*, 2000.
- [5] P.A.E.M. Janssen, *J. Phys. Ocean.* 33 (2003) 863.
- [6] A.R. Osborne, *Mar. Struct.* 14 (2001) 275.
- [7] M. Onorato, A.R. Osborne, M. Serio, and S. Bertone, *Phys. Rev. Lett.* 86 (2001) 5831.

- [8] Andonowati, N. Karjanto and E. van Groesen, Extreme wave phenomena in down-stream running modulated waves, submitted to Applied Mathematical Modelling (2004).
- [9] E. van Groesen, Andonowati, and N. Karjanto, Deterministic properties of nonlinear modulation instability, Proc. Rogue Waves 2004, Brest, France.
- [10] E. van Groesen, Andonowati, and N. Karjanto, Displaced phase-amplitude variables for waves on finite background; submitted PLA.
- [11] E. van Groesen and Andonowati, Periodic wave signals of extreme crest height, in preparation.
- [12] Andonowati and E. van Groesen, J. Nonlinear Opt. Phys. Material 12 (2003) 221.
- [13] Craig et. al. submitted to Phys. of Fluid, 2005.
- [14] E. van Groesen and E.M. de Jager, Mathematical structures in continuous dynamical systems, North Holland, Elsevier, Amsterdam, 1994.